Title: Microfabricated probes for studying brain chemistry: a review

Authors: Thitaphat Ngernsutivorakul; Thomas S. White; Robert T. Kennedy

To be cited as: ChemPhysChem 10.1002/cphc.201701180

Link to VoR: https://doi.org/10.1002/cphc.201701180

Review: Microfabricated Probes for Studying Brain Chemistry

Authors: Thitaphat Ngernsutivorakul[a], Thomas S. White[b], and Robert T. Kennedy*[ac]

a. Department of Chemistry, University of Michigan, 930 N. University Ave, Ann Arbor, MI 48109
b. Macromolecular Science and Engineering, University of Michigan, 3003E, NCRC Building 28, 2800 Plymouth Rd., Ann Arbor, MI 48109
c. Department of Pharmacology, University of Michigan, 1150 W. Medical Center Drive, Ann Arbor, MI 48109
*Corresponding author, Email: rtkenn@umich.edu

Table of contents (graphic and text)

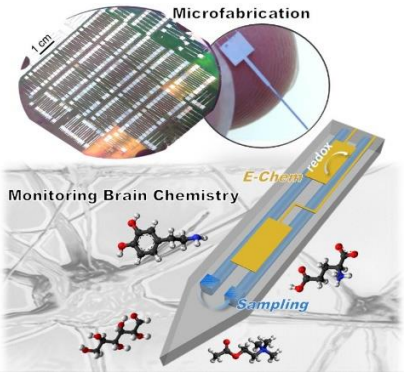

Microfabricated neurochemical probes: Microfabrication technology emerges as an important tool for developing miniature, high precision probes for electrochemical detection and sampling from live brain tissues. This review describes advances and perspectives in adapting microfabrication to create the next generation of neurochemical probes.

Acknowledgement

This work was supported by NIH R37 EB003320. The images in Figure 2, Figure 3B & 3C, and Figure 4C & 4D are adapted with permission from the references cited in the figure legends. We also fully acknowledge the authors and the original sources of Figure 4A & 4B.

Keywords

Neurochemistry, Microfabrication, Microdialysis, Electrochemical sensors, Neural probes

Conflict of Interest

The authors declare no competing financial interest.

Abstract: Probe techniques for monitoring in vivo chemistry (e.g., electrochemical sensors and microdialysis sampling probes) have significantly contributed to a better understanding of neurotransmission in correlation to behaviors and neurological disorders. Microfabrication allows construction of neural probes with high reproducibility, scalability, design flexibility, and multiplexed features. This technology has translated well into fabricating miniaturized neurochemical probes for electrochemical detection and sampling. Microfabricated electrochemical probes provide a better control of spatial resolution with multisite detection on a single compact platform. This development allows the observation of heterogeneity of neurochemical activity precisely within the brain region. Microfabricated sampling probes are starting to emerge that enable chemical measurements at high spatial resolution and potential for reducing tissue damage. Recent advancement in analytical methods also facilitates neurochemical monitoring at high temporal resolution. Furthermore, a positive feature of microfabricated probes is that they can be feasibly built with other sensing and stimulating platforms including optogenetics. Such integrated probes will empower researchers to precisely elucidate brain function and develop novel treatments for neurological disorders.

Table of Contents

Biographical Sketch

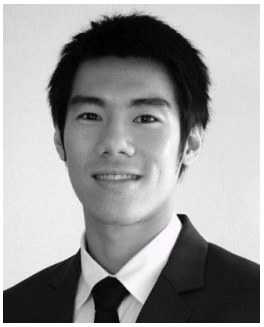

Thitaphat (Non) Ngernsutivorakul received his B.S. / M.A. in Chemistry from the University of Virginia in 2012. He is completing his Ph.D. at the University of Michigan, under the guidance of Dr. Robert T. Kennedy. His research involves using microfabrication for miniaturization and enhancement of chemical analysis systems. He is currently working towards developing next generation of microfabricated sampling probes with integrated analytical systems for monitoring brain chemicals at high spatiotemporal resolution.

Thomas S. White is currently a Ph.D. student in the Macromolecular Science & Engineering Program at the University of Michigan. He graduated from Central Michigan University in 2016 with a B.S. in Mechanical Engineering. In the spring of 2017, he joined the Kennedy research team. His current work focuses on microfabricated probes for neuroscience applications. Other research interests include optogenetics, polymers, MEMS, and nasal drug delivery.

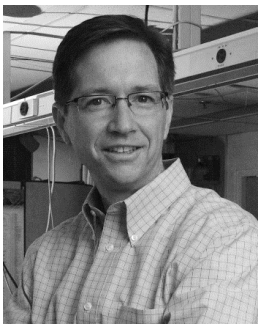

Robert T. Kennedy earned his Ph.D. in 1988 at the University of North Carolina and is presently the Hobart Willard Distinguished University Professor of Chemistry at the University of Michigan. His research focuses on bioanalytical chemistry including development of microfluidics, liquid chromatography, capillary electrophoresis, and mass spectrometry for studying hormone and neurotransmitter secretion, high-throughput screening, and biomolecular interactions. He has been adviser to over 60 graduate students and 30 post-doctoral scholars. He has received several honors for his research including most recently the ACS Chromatography Award and the Ralph Adams Bioanalytical Chemistry Award.

1. Introduction

Brain chemicals are highly diverse. Over two hundred different compounds have been identified as neurotransmitters, including amino acids, peptides, purines, lipids, monoamines, and other small molecules (e.g., acetylcholine)[1,2]. These chemicals participate in neural activity and are involved in various physiological functions, such as learning, memory, mood, and movement[3–5]. Abnormal levels or dynamics of neurotransmitters also link to mental illnesses and neurological disorders, such as Alzheimer's[6,7] and Parkinson's diseases[8–11]. It is therefore of interest to study dynamics of neurotransmitters and their metabolites in the brain extracellular space. Besides these compounds, other chemicals including metabolic intermediates and drugs are also important for brain functions. Energy metabolites (e.g., glucose and lactate) provide fuel for neurons[12], and measuring their concentrations has proven useful for diagnostics in traumatic brain injury[13–15]. Drugs or psychopharmacological substances can have effects on neurotransmission in many different ways, such as enhancing or inhibiting transmitter release[16].

Measuring brain chemistry in vivo has proven indispensable in better understanding chemical neurotransmission, which can be correlated to brain functions, behavior and pharmacology[16–20]. Probe techniques, such as electrochemical sensors[21–23] and microdialysis sampling[24–28], have remained predominant for in vivo neurochemical monitoring. In these techniques, needle-like probes are implanted into live brain tissues for direct chemical measurements. These techniques are used in many fundamental neuroscience studies[29–34]. They have also been translated into clinical settings, e.g., using electrochemical sensors during deep brain stimulation surgery[35–37], and using microdialyis probes in neurocritical care units[15,38–40]. First generation probes were typically handmade and have several limitations, including variability, low reproducibility, and limited design flexibility. The probe size can be bulky for the sampling probes in particular, leading to poor spatial resolution and substantial

tissue damage.

Several efforts have been devoted to using microfabrication for overcoming the above limitations. Microfabrication techniques ultimately allows development of miniature, multiplexed and highly-precise probes for studying brain chemistry. Other advantages also include a wide choice of materials, scalability, and batch fabrication. Furthermore, microfabrication offers unique opportunities for incorporating multiple functions into a single probe, such as electrophysiological recording, drug delivery, and optical stimulation. In this review, we aim to provide a background and an overview of microfabricated probes for monitoring brain chemistry. We will discuss different approaches relevant to probe development for electrochemical detection and sampling. Assays coupled to sampling probes for neurochemical monitoring with improved temporal resolution will also be discussed. Lastly, microfabricated optical elements for optogenetics that are of particular interest to neurochemical probes will be highlighted.

2. Background: In vivo monitoring technology

Criteria for evaluating methodology for in vivo neurochemical monitoring include sensitivity, selectivity, spatial resolution, temporal resolution, and multiplexing[23,25,41–44]. Sensitivity and selectivity are crucial to neurochemical measurements as the brain extracellular space is a complex mixture of chemicals with concentrations from picomolar (pM) to millimolar (mM). Spatial resolution is important due to the heterogeneity and small size of the brain structures. Temporal resolution is essential because neurochemical levels can alter rapidly (i.e., on millisecond time scale during exocytosis[45,46] or second time scale during behavior or stimuli[47–50]). Finally, simultaneous measurement of multiple chemicals is often needed when one would like to study multiplexed transmission or interactions between neurotransmitters, metabolites and drugs[51]. Therefore, it is desirable to develop technology that allows multiplexed neurochemical monitoring with long-term stability and high spatial and temporal resolution. In vivo neurochemical monitoring has been performed by non-invasive imaging techniques, such

as positron emission tomography (PET), functional magnetic resonance spectroscopy (fMRS), and genetically-encoded biosensors, or by invasive techniques, such as electrochemical sensors and sampling methods, that involve probe insertion into brain tissue. Strengths and weaknesses of each monitoring technique are summarized in Table 1.

Non-invasive imaging techniques. Predominant neurochemical imaging techniques include PET and fMRS. In PET, radioactive tracers (i.e., positron-emitting radionuclides) are intravenously injected into the bloodstream for labeling interested molecules in the brain prior to scanning[52–54]. Even though this technique is highly effective, it has limited spatial (2 - 3 mm at state of the art[55,56]) and temporal resolution (several seconds to minutes)[57–59]. fMRS uses a magnetic field to resolve ^{1}H spectra for identification and measurement of brain chemicals[60,61]. This technique has spatial[61] and temporal resolution[62–64] within the scales that are comparable to those of PET. The advantage of fMRS mainly stems from its non-requirement of tracers, but this technique suffers inherently poor sensitivity. Although administration of a contrast agent may improve sensitivity, it still remains insufficient for detecting many neurotransmitters at basal concentration.

Imaging brain chemicals via genetically-encoded biosensors is an emerging technology based on introduction of fluorescent markers into the tissue of interest[65–67]. This technique allows chemical measurement with superior spatial (μm-scale) and temporal resolution (ms to s). Despite this advantage, this technology is still in its infancy. Thus far only glutamate can be studied in vivo by this approach with a sub-micromolar (μM) limit of detection (LOD). Engineering a marker to efficiently yield a fluorescent signal for a specific molecule is also a long and difficult process. Due to several limitations of the imaging techniques, the probe techniques remain popular for in vivo neurochemical monitoring.

***Electrochemical sensors*.** Electrochemical detection of neurotransmitters relies on use of microelectrodes. Commonly, a microelectrode is made by aspirating a carbon fiber or a metal wire (~10 μm diameter) into a glass capillary before pulling the glass capillary and manually

trimming the electrode site to a length of 50 - 100 µm (Figure 1A). Using electrochemical methods[23,68], such as amperometry or fast-scan cyclic voltammetry (FSCV), electroactive molecules (e.g., dopamine and serotonin) can be detected directly via a redox reaction at the exposed electrode site. For detection of non-electroactive molecules (e.g., glutamate and glucose), the surface of electrode is treated with a selective enzyme/ membrane to generate an electroactive product[69,70], such as H_2O_2 via oxidase reaction, or nicotinamide adenine dinucleotide (NADH) via dehydrogenase reaction. Microelectrodes can allow in vivo monitoring with high spatial (10 - 100 µm) and temporal resolution (ms to s). Due to this advantage, electrochemical sensors are popularly used for real-time monitoring of transient neurochemical changes during behavior and/or stimulation. Selectivity, sensitivity, and LODs of the electrochemical sensors rely on several factors, such as electrode design, materials for electrode and selective-membrane, fabrication procedures, and detection method. Advances in technique and instrumentation, better control of electrode surface chemistry, and development of new materials and methods for electrode modification have improved overall selectivity and sensitivity. This improvement has allowed detection of several neurochemicals with low LODs (e.g., below 500 nM for glutamate[71], and below 20 nM for dopamine[72,73]).

Development of microelectrode arrays has become a topic of interest since it allows study of networks and chemical heterogeneity[74] within singular closely-spaced brain regions. Furthermore, the multisite platform can be useful in multiplexed monitoring if each electrode has a different selectivity. Traditionally, multisite in vivo monitoring may be performed by implanting several individual microelectrodes with the aid of a stereotaxic system for manual alignment[75]. An alternative approach is to create electrode arrays either by bundling of microwires or placing carbon fibers into multi-barrel pulled glass capillaries[45,76]. Although these two approaches seem to be effective, they have limitations in term of reproducibility and spatial control. Scalability has remained a challenge. Simultaneous recording at vertically-spaced different spots is also not

possible highlighting the inflexibility of design of manually prepared electrodes. Several efforts have used microfabrication to overcome these problems (discussed in Section 3).

Sampling methods. Microdialysis is a popular sampling method for in vivo studies. In microdialysis, an implantable probe (Figure 1B) is constructed by sheathing inlet and outlet capillaries with a hollow-fiber, semi-permeable membrane which is plugged at one end (220 - 500 µm in diameter, 1 - 4 mm long)[25–27]. During sampling, the inlet is infused with a buffer that matches the ionic composition of extracellular fluid at 0.1 - 3 µL/min. Sampling occurs at the membrane where analytes are extracted from the extracellular space according to their concentration gradients. The buffer with extracted analytes, called dialysate, is collected in fractions before chemical analysis with an appropriate analytical technique. Microdialysis sampling is widely used for in vivo chemical monitoring due to its versatility and feasibility for coupling to various analytical techniques[43,77], such as liquid chromatography with mass spectrometry (LC-MS), immunoassay, and capillary electrophoresis with laser-induced fluorescence (CE-LIF). This feature allows measurement of any neurochemicals and drugs with high sensitivity and selectivity, and multi-analyte capability.

An inherent weakness of microdialysis sampling is poor spatial resolution due to a large size of membrane tubing, which correlates to an active sampling region. An alternative sampling method with higher spatial resolution is miniaturized push-pull sampling or "low-flow push-pull perfusion"[78,79]. In this approach, the probe (Figure 1C) is constructed by mounting two 20 µm inner diameter (i.d.)/ 220 µm outer diameter (o.d.) fused-silica capillaries side-by-side, then sheathed with a 180 µm i.d./ 220 µm o.d. polyimide tubing. Sample is pulled from one capillary using low flow rates (typically at 50 nL/min) and a make-up fluid is pushed from another capillary at the same flow rate. The push-pull probes consequently sample only from the probe tip, resulting in substantially better spatial resolution, as compared to microdialysis probes. However, the overall size of the push-pull probe remains bulky due to the assembly process. This large size precludes experiments in many small brain regions. It can also cause tissue

damage that may confound measurement in vivo[80]. To address the size limitation in sampling probes, recent efforts have resorted to microfabrication. Another traditional weakness of the sampling methods is poor temporal resolution (order of mins); however, advancement in analytical methods and microfluidic technology has allowed in vivo neurochemical monitoring with temporal resolution of less than 10 s. These subjects will be discussed further in Section 4.

3. Microfabricated electrochemical probes

The field of neuro Microelectromechanical Systems, or "neuroMEMS" (see historical reviews and recent technological advancement[81–84]) has well-established technologies for fabricating neural probes to investigate electrical activity at multiple different sites. Advancement in microfabrication tools and materials allowed development of small, highly reproducible, highly integrated, and high density neural probe arrays (see [81,85] for an example of 256-site probes; a recent work has shown a neural probe with 1356 sites[86]). The microfabrication process has more recently been adopted to construct probes with sensor arrays for neurochemical recording. Careful considerations of material for substrate and electrodes, and surface architectures are required to achieve desired performance[87]. Different approaches with their key parameters in microfabricating neurochemical probes are summarized in Table 2[88–103].

Electrodes. A key component in electrochemical detection is the electrode site. By microfabrication, electrodes can be deposited as thin films (less than a few hundred nm) by various techniques, such as sputtering, low pressure chemical vapor deposition (LPCVD), and plasma-enhanced chemical vapor deposition (PECVD) prior to insulation. Choices of materials for insulating the electrodes include silicon dioxide, low-stress silicon nitride, SU-8, polyimide, and parylene. For detection of the H_2O_2 product from enzyme sensors, Pt is normally used due to its electrocatalytic property, long-term biocompatibility, and ease of fabrication. For direct detection of electroactive molecules (monoamines in particular), carbon is a more suitable material because it has less charging current, more favorable electrocatalytic properties for

these molecules, and relatively wide potential window. Since direct deposition of carbon (i.e., via sputtering or evaporation) typically resulted in low-quality film, it is preferable to use pyrolysis of photoresists in the microfabrication of carbon electrodes[93,104]. The surface area of an electrode is also another important parameter in designing neurochemical probes. Enlarging this surface area increases sensitivity; however, a large surface area can increase probe size and compromises spatial resolution. As seen in Table 2, electrode surface areas ranged from 500 - 1000 μm^2 for direct electrochemical detection of dopamine, and 5000 - 10000 μm^2 for detection of non-electroactive species by enzyme-coated electrodes. The gap between electroactive sites was typically kept at 50 – 200 µm to limit cross-talk. Increasing surface roughness without significantly changing overall size would be an approach to improve sensitivity for a given size electrode. Strategies for surface enhancement include coating electrodes with porous materials, such as conductive polymers[105–107], carbon nanotubes[108–110], graphene composites[111–113], and durable platinized Pt[114].

Surface modification of electrodes, with selective membranes, is generally required to improve selectivity and sensitivity. For detection of non-electroactive molecules, enzymes mixed with bovine serum albumin (BSA) are typically immobilized on electrodes by crosslinking with glutaraldehyde. Thickness of the enzyme coating is critical to performance of the electrode as the substrates and products must move through the membrane layers. Excessive thickness could lead to slow response time[115] of the electrode and higher degree of cross-talk between electrodes[116]. On the other hand, overly thin membranes may lead to insufficient sensitivity and non-uniformity; that could be detrimental to stability and reliability of the electrode. Therefore, the thickness of the membrane should be well-controlled and optimized. For example, the enzyme thicknesses on the microfabricated electrodes were reported to be approximately 5 – 10 µm thick[91,99]. Rise times of the microfabricated electrodes ranged from ~1 – 8 s (see Table 2). Besides thickness, other factors can also affect to analytical performance and response time of the electrode, including the amount of immobilized enzyme which related to deposition

procedures. For enzyme immobilization, small volumes of enzyme solutions were dispensed directly on microfabricated electrode sites using a microsyringe with the aids of microscope and micromanipulator[89,99]. Alternatively, electrochemically aided adsorption was adapted for enzyme coating at high-spatially control, enabling parallel depositions of different enzymes at closely-spaced electrodes[91]. Microfabrication techniques (i.e., lithographic patterning of polymers/ resists) also made it possible to create microwells which encompassed the planar electrodes. Not only did these microwells act as an effective insulator, but they also allowed precise immobilization and stable formation of the selective membranes[94,102,117].

Additionally, several types of polymers[118] have been explored in microfabrication of neurochemical probes, in order to reject interference and prevent surface fouling. Common deposition methods included dip-coating and electropolymerization. Nafion[88,96] or overoxidized polypyrrole[89] can be used for rejection of anionic molecules, such as ascorbic acid, 3,4-dihydroxyphenylacetic acid (DOPAC) and homovanillic acid (HVA), while promoting adhesion of cation molecules, like catecholamine. Phenylenediamine derivatives are particularly useful for detection of H_2O_2 product[94,95]. These polymers prevent access of large molecules (including ascorbic acid and dopamine) while allowing fast response and high selectivity of the smaller H_2O_2 molecules. Furthermore, (3-aminopropyl)triethoxysilane (APTES) can be used to improve storage and functional lifetime and reproducibility of enzyme adhesion[91].

Stiff probes. Si is the most widely used substrate due to its mechanical and electrical properties, and relatively simple processing. Standard lithography allows patterning of microprobe structures and recording sites with fine features. Wet etching or dry etching, particularly deep-reactive ion etching (DRIE) based on the "Bosch process"[119], are employed in defining probe outlines and releasing probes[120]. To precisely limit probe thicknesses, a boron-doped layer[121] or a silicon-on-insulator (SOI) wafer[122,123] may be used as an etch stop. These approaches have ultimately allowed fabrication of very thin neural probes (less than 15 μm) with precisely-defined tapered tip (for example, see[124]). Alternatively, a combined process of DRIE

and wafer grinding can be used in thinning a Si neural probe down to 25 μm[125,126]. Different designs of microfabricated Si probes have been developed by several groups for monitoring several neurochemicals, including dopamine[88,93], glutamate[89–91], lactate and glucose[94] with LODs of sub-μM. In all of these probe designs, at least 4 electrode sites were integrated on a single probe, enabling concurrent recording of a target analytes at high spatially different locations. For example, the microfabricated probes were employed in recording stimulated dopamine in 4 different sites (at 100 – 200 μm vertically spaced) in rat striatum by FSCV[93] or amperometry[88]. These results revealed heterogeneity of the stimulant effect on dopamine release, indicating necessary use of the microfabricated probes. With multi-site probes, simultaneous detection of multiple analytes in different target areas could also be achieved precisely[91,94]. At an additional electrode site, direct integration of a reference electrode can be performed via electrodeposition[90,91]. Further, parallel electrophysiological recording was also made feasible by adding extra electrodes[88,95]. Figure 2A shows an example of a single probe consisting of 8 electrochemical sites (60 μm × 125 μm) and 6 electrophysiological sites (15 μm diameter). This microfabricated probe was used for concurrent recording of glutamate and electrophysiology at multiple sites in rat striatum.

Other types of stiff substrates for microfabricating neurochemical probes have also been explored. The Gerhardt group has extensively developed probes with electrode arrays based on 125 μm thick ceramic wafers[127]. Probe shapes with ultra-fine tip were created by using a diamond dicing saw and a laser cutter. Although thinner ceramic wafers (25 – 50 μm) were also commercially available, they were too fragile and difficult to process. The ceramic-based probes were treated with specific enzymes for monitoring glutamate[96,97], lactate[98], choline, acetylcholine[99], and glucose (for example, see Figure 2 B)[100]. A self-referencing recording approach was also used to remove interferents[128]. Chronic measurements in freely moving animals were also demonstrated with adequate sensitivity and selectivity, illustrating a potential advantage of biocompatibility with this substrate[129].

Polymer probe. Interest in developing neural probes using "soft" materials like polymers, has recently grown as matching the Young's modulus of the probe material to the soft brain is thought to minimize tissue damage[106,130–132]. Choices of traditional soft materials included polyimide, SU-8, parylene, and polydimethylsiloxane (PDMS). Emerging polymer materials, namely shape memory polymers, have also gained attention in recent years due to their capability to adjust Young's modulus based on temperature changes[133–135]. Therefore, these substrates may be tailored to be sufficiently stiff during probe insertion and softened inside the tissue. Despite the potential benefit of soft implants, they are generally designed for primary use at the brain surface, or at depths up to a few millimeters. Otherwise, soft implants normally require the use of needle guide or stiff coating (such as polyethylene glycol (PEG)[136,137] or biodegradable silk[138,139]) for aiding tissue penetration and trajectory to deep brain tissue.

Thus far only a few studies have been reported on using polymeric substrates to microfabricate neurochemical probes[101,102]. One attempt was to microfabricate polyimide-based probes for detecting glutamate and lactate[102] (Figure 2C). The polymer probe consisted of Pt electrodes with integrated reference and counter electrodes. The final probe size was 500 µm wide × 100 µm thick, and 5.5 mm or 16 mm long. Utility of the more durable probe (5.5 mm long) was demonstrated in vivo by monitoring glutamate in rat cortex at 1.7 mm depth.

Microfabrication has allowed construction of multi-site electrodes at high-spatially spaced positions. However, the total sizes of microfabricated probes are still larger than a single carbon fiber electrode. Alternatively, one interesting approach was to combine processes of carbon fiber assembly and microfabrication[103]. This approach used a glass microgroove mold for manually aligning 8 carbon fibers to a printed-circuit board before applying photoresists to protect the fiber tips. 10 device sets were attached on a 100 mm diameter Pyrex wafer for subsequent microfabrication processes, including chemical vapor deposition (CVD) of parylene to isolate electrodes. After release of the devices, the fibers were manually trimmed to a length of 50 – 200 µm. The resulting 8-shank carbon fiber array had 9 µm diameter footprint for each

electrode (Figure 2D). PEG was used to stiffen the fibers prior to probe insertion followed by FSCV recording of dopamine in rat striatum. In essence, this approach appears to be a relatively simple fabrication method for multi-site electrodes with subcellular diameter. However, device design and size accuracy were still limited due to some manual processes. Incorporation of automated tools and microfabrication techniques, such as plasma etching, could improve design flexibility, scalability, and overall uniformity of the finalized probe arrays.

Conclusions. Microfabricated electrochemical probes have enabled neurochemical monitoring on multiple sites with high-precision spatial control. Other advantages include scalability and feasibility to generate a multiplexing sensor or a parallel platform for simultaneous chemical and electrophysiological recordings. Similar electrical components may also be adapted to perform other functions, such as pH and oxygen sensing[140], and electrical stimulation[141,142]. Furthermore, microfabrication will open an opportunity for monolithic integration of electrochemical probes with microfluidic and optical modalities (see below). A variety of substrates and materials has been used in development of the microfabricated probes with the goal of creating small, biocompatible devices with enhanced sensor sensitivity and selectivity. However, the current technology still has a limitation in a number of measurable neurochemicals (less than 10 compounds can be measured). Future advancements in nanochemistry, materials, surface engineering and coating technologies may prove useful to broaden performance of the next generation probes. Utility of microfabricated probes have mostly been demonstrated only for acute studies. Future work in chronic studies will help to evaluate long-term stability and robustness of these chemical sensors.

4. Microfabricated sampling probes

Microfabrication has been employed to embed microfluidic channels into neural probes[143–145]. Small channels with different shapes and material types can be constructed by a variety of techniques, such as surface micromachining using sacrificial layer, and bulk

micromachining using buried channel technology[146,147] or wafer bonding. Using microfabrication technologies, various microfluidic neural probes have been developed for neurological studies and treatments. Their features as well as manufacturing processes are well summarized in a recent review by Sim et al[148]. Most of the work in microfabricating fluidic probes aimed to improve microinjection or chemical delivery to brain tissues. These advancements also highlighted viable integration of the microfluidic features with in vivo electrophysiological recordings[145,149,150]. Nevertheless, similar microfabrication technologies can be adapted to fabricate sampling probes for neurochemical monitoring.

Push-pull/ direct sampling. Over the past few years, our group has developed the first, functional sampling probes for in vivo monitoring of brain chemistry[151]. Based on the buried channel technology, microfabrication in Si was used to construct push-pull sampling probes with 20 µm diameter channels. The microfabricated push-pull probes are 85 µm wide × 70 µm thick × 11 mm long, consisting of two 20 µm orifices at the probe tip for push-pull sampling (Figure 3A,i). The overall size of the microfabricated probes was 6-fold smaller than the capillary-based probes, thus potentially reducing tissue damage. Sampling at 50 nL/min from rat striatum, the microfabricated push-pull probe was coupled to a benzoyl-chloride LC-MS assay for monitoring of multiple neurotransmitters and metabolites. Assuming that the active sampling area of push-pull sampling is based on the space between the two orifices, the sampling area of microfabricated push-pull probe is estimated to be ~1200 μm^2. This sampling area is comparable to that of microelectrodes, as described above. In addition, microfabrication has allowed fabrication of additional channel without increasing overall probe dimension (Figure 3A, ii). This additional channel can be further used for microinjection or sample preparation steps.

Other groups have recently also investigated microfabrication of sampling probes. Besides sampling, other features were further implemented in these probes. One such probe was a silicon-based probe designed for sampling with three integrated electrodes for sensing[152]. Another work showed a probe that contained microfluidic channels for sampling as

well as electrodes for stimulating and recording in one package[153] (Figure 3B, i). This probe was constructed by polyimide and SU-8. The resulting shank size of 240 µm wide × 86 µm thick. Through a single inlet, direct sampling was performed at 300 nL/min without adding a makeup fluid into the sample. In vitro tests revealed the probe capable of segmented-flow sampling (Figure 3B, ii), on-chip detection, and functional electrical capabilities. Both designs sought to miniaturize sampling probes with integrated functions through microfabrication techniques. However, it remains to be determined how these probes will function for monitoring neurochemicals in vivo.

Membrane integration. Although microfabricated push-pull probes allow sampling with high spatial resolution, they are more susceptible to clogging than microdialysis probes due to the absence of membranes. Proteins and debris that enter the sampling channels may also interfere with the downstream analytical assays. Integration of nanoporous membranes into the miniaturized sampling probes can be performed to circumvent these potential issues. A wide variety of techniques has been used to fabricate nanoporous membranes[154], including ion-track etching[155], focused ion beam drilling[156], and rapid annealing[157]. However, these membranes are designed for integration on microfluidic devices rather than microprobe structures. Embedding membranes in microfluidic neural probes is challenging because 1) the small support structures may lead to collapse of the membrane during fabrication, and 2) the limited surface area increases the difficulty of membrane attachment. Membranes should also contain sufficient porosity to allow suitable extraction efficiency/ recovery of analytes while having sufficient strength to avoid rupture as fluid infuses into the microchannels.

Zahn et al has reported microfabrication of dialysis probes[158]. Preliminarily, a permeable polysilicon (100 nm thick with 5 – 20 nm pore defects) was fabricated on top of a 10 µm tall × ~150 µm wide channel. Although the membrane was successfully formed over the channel, according to the authors, the thin membrane was too fragile to be effectively used. An alternative approach was to employ a sacrificial oxide spacer layer in creating 30 nm diffusion

passage, sandwiched between two layers of lithographically-patterned porous membranes (2 µm pores with a total thickness of 2-3 µm). Even though this probe proved its utility for in vitro sampling of a fluorescent dye, its capability for in vivo neurochemical sampling has not been tested. The membrane also had low porosity (i.e., 1.5%) which may limit recovery. The narrow flow passage may potentially lead to stiction issues[159]. Nevertheless, this pioneering work suggested possibility of miniaturization of dialysis sampling probe.

Recently, our group has adapted nanoporous anodic aluminum oxide[160–162] (AAO) to microfabricate Si probes for in vivo microdialysis[163] (Figure 3C). The AAO process was an attractive approach because it yielded straight nanopores with high density and controllable pore sizes. The process was also relatively simple, inexpensive, and compatible with the process flow for Si microfabrication. In our approach, a 400 nm thick layer of AAO with pore sizes of 50 - 70 nm was used as a mask for DRIE through 2 µm thick Si microchannels. The AAO mask was removed before a 3 µm thick AAO was then fabricated over the porous Si channels in order to provide sufficient mechanical strength. The final probe size was 180 µm wide × 45 µm thick × 11 mm long, containing a 30 µm tall × 60 µm wide U-channel. The probes yielded 2 - 20% relative recovery at a perfusion rate of 100 nL/min. Coupling to an LC-MS assay, utility of the probe was demonstrated in vivo by monitoring 14 neurochemicals at basal concentrations. Compared to the conventional probe, the microfabricated probe had 6-fold smaller surface area of sampling, thus providing improved spatial resolution. Our ongoing work is to optimize morphology of the membranes so that they permit better recovery and can withstand higher pressure. Improvement in recovery would lead to increase the number of detectable analytes as well as potentially reducing sampling areas. Stronger membranes would allow device operation at smaller channel sizes. Therefore, the probes can ultimately be made smaller with future improvements in membrane performance. As the AAO process allows alteration of membrane pore sizes, different molecular weight cut-off limits can also be explored.

Assays for improved temporal resolution. In sampling techniques, temporal resolution is limited by mass sensitivity and throughput of analytical methods coupled to the sampling probe[28,77]. Particularly, the use of low flow rates (< 100 nL/min) in the microfabricated sampling probes can compromise temporal resolution as a long period is required to collect enough sample volume for the subsequent assay. For instance, to collect 1 - 2 µL fractions for a conventional LC-MS assay, temporal resolution was limited to 20 min[151,163]. Miniaturized analytical methods, such as microbore LC or CE, may be utilized for improved temporal resolution. However, as samples travel from probes to analytical system, the temporal resolution is also limited by broadening of concentration zones due to Taylor dispersion[164]. This reduction in temporal resolution depends inherently on flow rates and capillary dimensions. The band-broadening may be mitigated by using high sampling flow rate (> 1 µL/min) and short, small-bore connecting tubing. As a result, temporal resolution of 3 - 30 s could be achieved[47,165–167]. In spite of this improvement, this approach was limited to only anesthetized subjects. It is also not suitable for the miniaturized probes where low sampling flow rates are required.

Another effective approach for improved temporal resolution is to use segmented-flow or droplet microfluidics[168–170]. In this approach, a sample flow is segmented into a train of discrete aqueous droplets by an immiscible fluorinated oil. By flow segmentation, sample droplets do not mix by diffusion during transport, and the temporal resolution is hence preserved. In vitro studies have shown that chemical sampling with sub-second time resolutions could be attained by using segmented flow[79,153,169]. Furthermore, droplet technology facilitates handling and manipulation of small-volume samples collected at short intervals. Integration with other microfluidic devices was also made feasible for further analytical procedures[171,172].

Analysis of droplets may be performed by a variety of high throughput analytical methods[173]. Particularly, suitable analytical techniques for neurochemical analysis of droplets included enzyme assay, microchip CE, and direct infusion ESI-MS. Low-flow push-pull perfusion with segmented flow was coupled to an enzyme assay for analysis of glutamate, with 7 s

resolution and a LOD of 300 nM[79]. Microchip CE with LIF detection was used for simultaneous measurement of amino acids in droplet dialysates with LODs of 80 - 100 nM[174,175]. By using an offline analysis, droplets could be generated at a high frequency (2 nL droplet at ~0.5 s interval) before pumping them into the chip at a slower rate. Each droplet was therefore analyzed without loss of temporal resolution although the separation time was 50 s. As a result, 9 s temporal resolution was achieved in vivo. Using ESI-MS assay, acetylcholine in dialysate droplets (160 nL at 5 s interval) was monitored with 5 s temporal resolution and a LOD of 5 nM[176]. In addition, choline and the acetylcholine esterase inhibitor were simultaneously detected. In principle, the MS assay offers the most versatile route to analyze droplet samples. This assay provides many advantages, such as high sensitivity and selectivity, label-free detection, and multi-analyte capability. In contrast to the CE assay, flow desegmentation prior to ESI-MS was also not necessary when using suitable oils and optimized flow rate and voltage[177]. Further, enhancement of MS sensitivity and reduction of matrix effects can be achieved by using nanospray ionization[178–180]. This approach has enabled compatibility of the assay with much smaller sample volume (i.e., analysis of < 5 nL droplets have been made possible), thus facilitating neurochemical sampling at low flow rates while providing high temporal resolution. Future optimization of the MS assay and advances in instrumentation would open opportunities for simultaneous monitoring of many more neurochemicals.

Conclusions. Microfabricated fluidic probes can accommodate not only localized drug delivery but also sampling for neurochemical monitoring. Two main types of the in vivo sampling techniques are push-pull perfusion and microdialysis. Push-pull perfusion probes provide high spatial resolution monitoring while microdialysis probes offer benefits of sample cleanup and ease of device operation. Comparing to traditional sampling probes, the microfabricated probes are at least several fold smaller, thus leading to improved spatial resolution and reduced tissue damage. Microfabrication facilitates direct integration of more channels and other functional components within the probes. Challenges in development of microfabricated sampling probes

typically include issues related to clogging and high backpressure due to the use of small microchannels. To overcome these problems, careful considerations in probe designs and materials are necessary. Even though utility of miniaturized sampling regions may limit extraction efficiency, versatility of the method allows coupling of the probes to highly sensitive analytical instruments for multiplexed detection of a variety of neurochemicals. Another limitation of the microfabricated sampling probes is poor temporal resolution due to a requirement of operating at low flow rates. Integration of the probes with a droplet-based microfluidic system in conjunction with a high throughput assay will be a key for future improvements in temporal resolution. Also, development of high-throughput assays that provide multiplexed measurements is key for this approach to have impact.

5. Potential for optical integration

Microfabrication already offers significant boons to neural probe research that have been discussed in previous sections of this review. Nonetheless, we feel significant room remains to extend the conversation to the topic of optogenetics[181–185]. The capacity to genetically prime and then optically stimulate isolated neuron clusters is particularly attractive for micron-scale probes designed to access small brain structures. Optogenetic experiments often employed optical fibers connected to a light source, such as a laser or LED, to supply the light sufficient for stimulation. Most studies have typically relied upon behavioral observation or electrophysiological recording to ascertain the effect of optically manipulating a particular circuit or group of neurons. However, these approaches do not evaluate neurochemical signaling or metabolic changes during stimulation, which is crucial to elucidate behavioral and neuronal effects. It is therefore important to couple direct neurochemical monitoring with optogenetics in order to provide a complementary view of neuron activities[186–188]. A combination of the two techniques has ultimately enabled new studies in neuroscience. For example, this approach accommodated the study of previously elusive causal link between specific patterns of

dopamine transmission and alcohol drinking behavior[188]. Despite utility and power of the coupled method, conventional probes made by assembly proved to be bulky and supplied poor spatial resolution. Microfabrication methods present a means to miniaturize the functions of larger probe designs while directly integrating optical elements into a single device. Reviews on optogenetics techniques have been published recently which outline the progress made in this field[189–192]. In this section, we select the particular work that may be beneficial to microfabricated neurochemical probes.

***Passive components*.** Direct integration of waveguides onto probe shanks presents the prospect of precise direction of light to neural circuits of interest. Materials such as silicon nitride, silicon oxynitride (SiO_xN_y), and photoresists have all been explored for their optical utility[193–198]. Efforts to expand the directional and wavelength mixing functionality of waveguides produced useful results[194–196]. Characterization tests of one probe revealed that light could be both separated by color and directed 90° from the shank in opposite directions[194]. In contrast, a separate project applied gradient index (GRIN) lenses to combine wavelengths along a single 30 µm wide × 7 µm thick waveguide tip and minimize heating effects (Figure 4A)[195]. In vivo experiments revealed distinctive neuron clusters could be simultaneously triggered by light wavelength, in the hippocampal CA1 region. Microelectrodes on the sampling area recorded different firing behaviors for each respective color. SU-8-based waveguides have also exhibited viability into in vivo testing (for example, see Figure 4B)[198,199]. Each probe relied upon an SU-8 waveguide (30 µm wide × 15 µm thick) and recording electrode, but one probe also included injection channels[199]. Both probes recorded neurological responses to light, however the drug injection port supplied a means to observe drug interactions during optical stimulation. SU-8 has shown merit as a viable optical material and may prove a cost effective alternative to physical vapor deposition (PVD) methods often required for nitride-based waveguides for some projects. Although SU-8 waveguides were relatively bulkier, they were easier to align with an external optical fiber to transfer light from the light source. The papers described here provide evidence

for the efficaciousness of waveguides. However, the waveguide approach typically requires wired-connection to external optical fiber and light sources, which may restrict physical movements of experimental subjects.

***Active components*.** As a significant portion of neurological activity occurs during free range movement, the ability to record brain activity under such conditions could further understanding of the relationship between neurochemical activity and behavior. To achieve this goal, several researches have gone into miniaturizing light sources for direct integration with neural probes. The Rogers Group developed flexible, multifunctional probes compatible with wireless systems for behavioral studies (Figure 4C)[200,201]. One flexible, PDMS-based probe, 500 µm wide x 50 µm thick, focused on microfluidic channels to complement µLED stimulation. Another design incorporated Pt sensing elements at total probe thickness of 20 µm. To aid insertion, the probes incorporated stainless steel and epoxy-based microneedles, respectively. In both cases, the probes provided optogenetic capabilities for the observation and manipulation of behaviors[157]. One probe enabled drug delivery, while the second allowed monitoring of both electrophysiology and temperature changes during optical stimulation. Histological studies revealed that tissue damage was negligible in both studies. The previous two examples show that softer probes can provide commendable performance during experiments. However, soft probes typically require a form of reinforcement as described.

The need for reinforcements illustrates the benefits of more rigid materials in neural probe fabrication. Silicon has seen considerable use in microfabrication processes and neural probe development. In particular, silicon-based probes can directly integrate sensing elements such as electrodes, waveguides, and miniaturized light sources, while offering ample stiffness to penetrate the brain. The micron-scale dimensions possible through microfabrication techniques can also reduce the likelihood of tissue damage. One approach involved fabrication and integration of bare laser diode chips (emitting at 650 nm) with a silicon neural probe[202,203]. The diode chips were directly coupled to SU-8 waveguides embedded on the probe shank, resulting

in a compact packaged device. This work demonstrates a potential feature of the miniaturized optical system for experiments in freely behaving animals; however, in vivo testing has not been reported. Some silicon-based probes have incorporated GaN μLED's on multiple shanks through microfabrication techniques[204,205]. GaN provides suitable emissive properties for blue wavelengths (450 - 460 nm) during channelrhodopsin-2 (ChR2)-based studies. Mutli-shank designs can facilitate a broader range of neural cluster stimulation per experiment. One example employed six, 100 μm wide x 40 μm thick x 3 mm long, shanks; each shank possessed 16 μLED's for 96 total optical elements in one array[204]. The 96 μLED probe permitted the simultaneous activation of multiple sites at various depths within mice neocortex regions. The direct integration of electrodes can allow more accurate quantification of neuron circuit firing through improved spatial resolution. In fact, a separate design contained 12 of μLED's (10 μm x 15 μm) distributed among 4 probe shanks (Figure 4D)[205]. Each shank (70 μm wide x 30 μm thick x 5 mm long) also employed Ti/Pt/Ir electrodes for electrical recording. During in vivo trials, multiple clusters of neurons were optically stimulated and recorded within the CA1 pyramidal layer of mice. The minimal wiring requirements also permitted the subjects free range movement during testing. The probes discussed here illustrate some of the versatility offered by μLED's in neurological studies. They open the door to free-range movement studies, flexible placement of light within different clusters of neurons, and low-power requirements which are compatible with wireless devices.

Conclusions. Optical stimulation of neurons opens new avenues for characterizing neurochemical changes. In this section, we have discussed both passive and active optical elements found in microfabricated neural probes. Waveguides made through microfabrication of silicon nitride or SU-8 can effectively direct light to specific regions of the brain. The integrated waveguide system can be tailored to deliver a variety of wavelengths facilitating a broader range of optogenetics studies. However, the waveguide system can be bulky, hindering experiments involved freely moving animals. This problem was the root motivation to using miniaturized

active optical components, which can be incorporated into different probe designs via microfabrication techniques. Particularly, the μLED approach is viable for scaling up and integration with other neural electrical interfaces. However, μLED's can be prone to heating issues, thus optimization in device design and optical parameters must be carefully evaluated. In addition, a significant portion of μLED-based probes appear to include only blue light wavelengths. Future advancements should also focus on a broader range of colors which would surpass the advantages offered by waveguides in this respect. As stated in earlier sections of this review, sampling probes allow versatility for monitoring various types of neurochemicals within target tissue areas. Electrochemical sensors offer rapid chemical recording in real time, but can focus only on a limited number of analytes. Microfabrication techniques will open up opportunities to integrate optoelectrical components with the two mentioned complementary monitoring techniques, resulting in an advanced probe with unprecedented degrees of multiplexing, spatial and temporal resolution, and applicability.

6. Summary and outlook

In vivo neurochemical monitoring is a vital tool for elucidating brain function and disease. Microfabrication technologies have enabled the possibility to create high density, highly-precise neural probes for studying brain chemistry. Development of microfabricated electrochemical probes enables multiplexed chemical measurement at high-spatially different brain locations. Microfabricated sampling probes allow neurochemical monitoring with minimal tissue damage and spatial resolution comparable to microelectrodes. With incorporation of flow-segmentation and advances in assay methods, it is also possible to achieve multicomponent chemical monitoring at sub-second temporal resolution. Notably, the microfabrication of neurochemical probes offers the potential to access different brain regions at high spatial control and at a size-scale that was previously impossible. The drive to perfect increasingly smaller designs, however, must be balanced with recording sufficient amounts of target analytes. In the case of

sampling probes, further considerations such as sample collection capability and practically-useful driving pressure, will also come into play. Nevertheless, we believe that future progress in analytical techniques and instrumentations will facilitate further miniaturization. Another exciting aspect of the microfabricated probes stems from their scalability and feasible integration with other neural interfaces, such as electrophysiology and optogenetics. The innovations in such multi-modal/functional probes will ultimately open opportunities for new discoveries in neuroscience.

Figure Legends

Figure 1. Schematic of conventional probes for in vivo neurochemical monitoring with comparison of probe sizes. A) Electrochemical microelectrode with 10 µm diameter, 50 µm long. B) Concentric microdialysis probe with 1 mm long polyacrylonitrile (PAN) membrane with 230 µm o.d. C) low flow push-pull probe made assembly of 20 µm i.d./ 90 um o.d. capillaries side-by-side, sheathed with 180 µm i.d./ 220 µm o.d. polyimide tubing. Models were drawn to scale for comparison of probe size and regions of chemical monitoring (at exposed electrode surface for (A), membrane surface for (B), and space between orifices for (C).

Figure 2. Examples of probes with multisite electrochemical sensors. A) Silicon probe for neurochemical monitoring (white rectangular) integrated with electrophysiological recording sites (small black dots)[95]. B) Ceramic probe for glucose recording[100]. C) Polyimide probe for glutamate recording[102]. D) Subcellular probe for dopamine detection made by combination of assembly of carbon fiber and microfabrication of parylene insulator[103].

Figure 3. Examples of microfabricated probes for sampling. A) Push-pull probe: orifices for sampling (A,i) and cross-section of a probe with additional channel (A, ii); B) Direct sampling probe, an arrow indicates a single sampling orifice (B,i). This probe is integrated with electrical recording and stimulation (circle dots), and flow-segmentation (B, ii)[153]. C) Dialysis probe: Top view of probe tip (C,i) with AAO membrane in the inset, and cross-section (C,ii) of a microchannel with embedded AAO-poly Si membranes[163].

Figure 4. Examples of microfabricated probes with optical elements. A) Neural probe with an oxynitride waveguide and iridium electrodes[195]. B) SU-8 waveguide, multi-shank probe for stimulation at varied depths[198]. C) Multilayered probe with microfluidic channels and µLED's[200]. D) Expanded view of µLED's from 4-shank probe design[205].

(All permissions were granted to reuse the images in Figure 2, Figure 3B & 3C, and Figure 4C & 4D. We included references to the original publications in the figure legends, and added a permission statement in the Acknowledgement. The images in Figure 4A & 4B have been distributed under a Creative Commons CC-BY license. These materials may be reused without obtaining permission from the publisher, providing that the author and the original source of publication are fully acknowledged.)

Figure 1

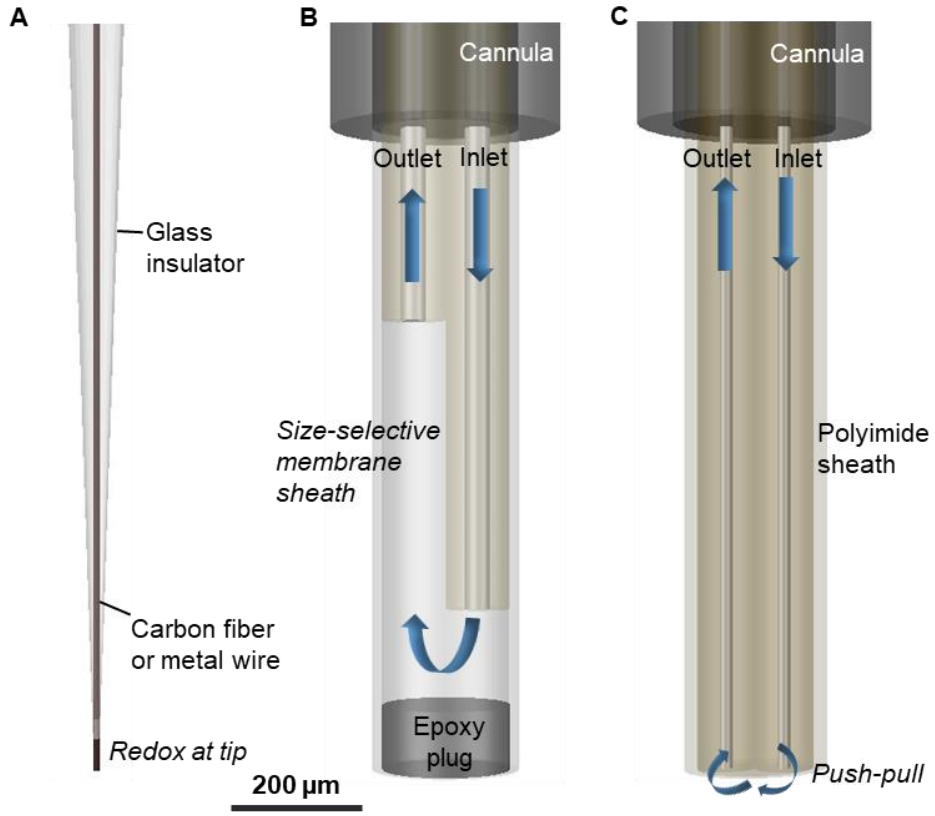

Figure 2

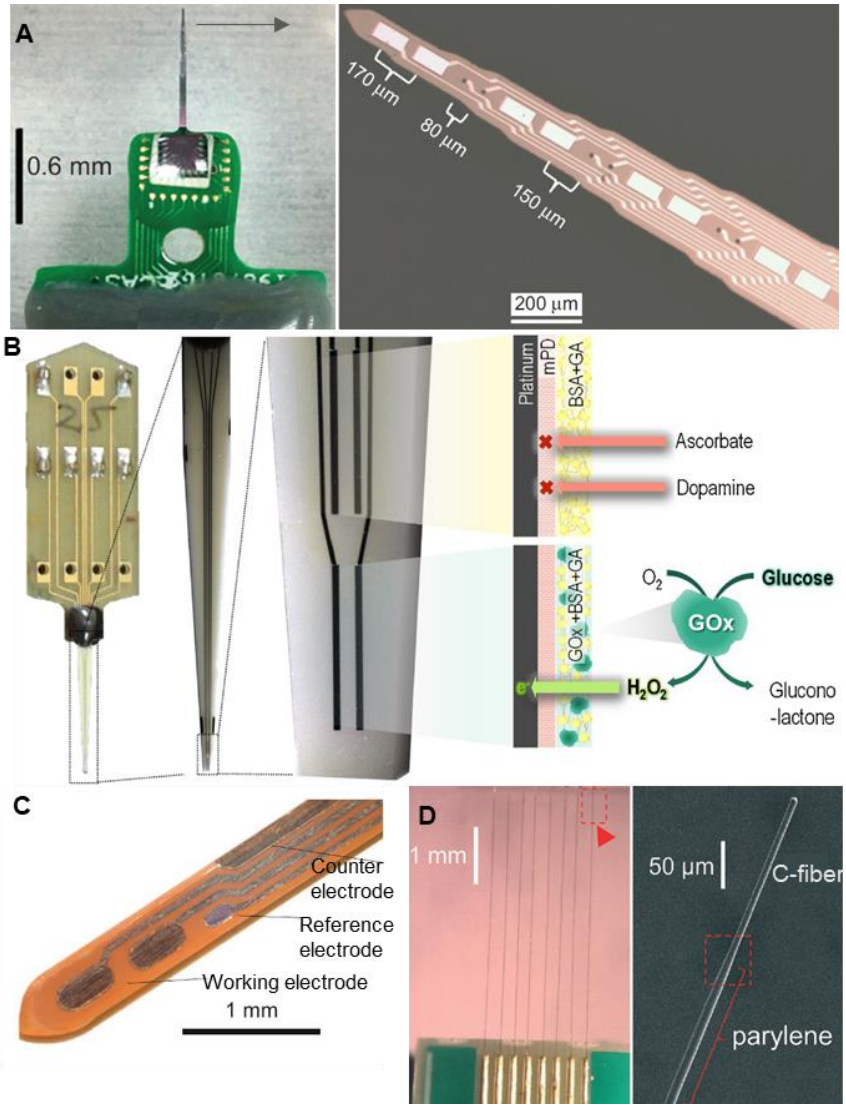

Figure 3

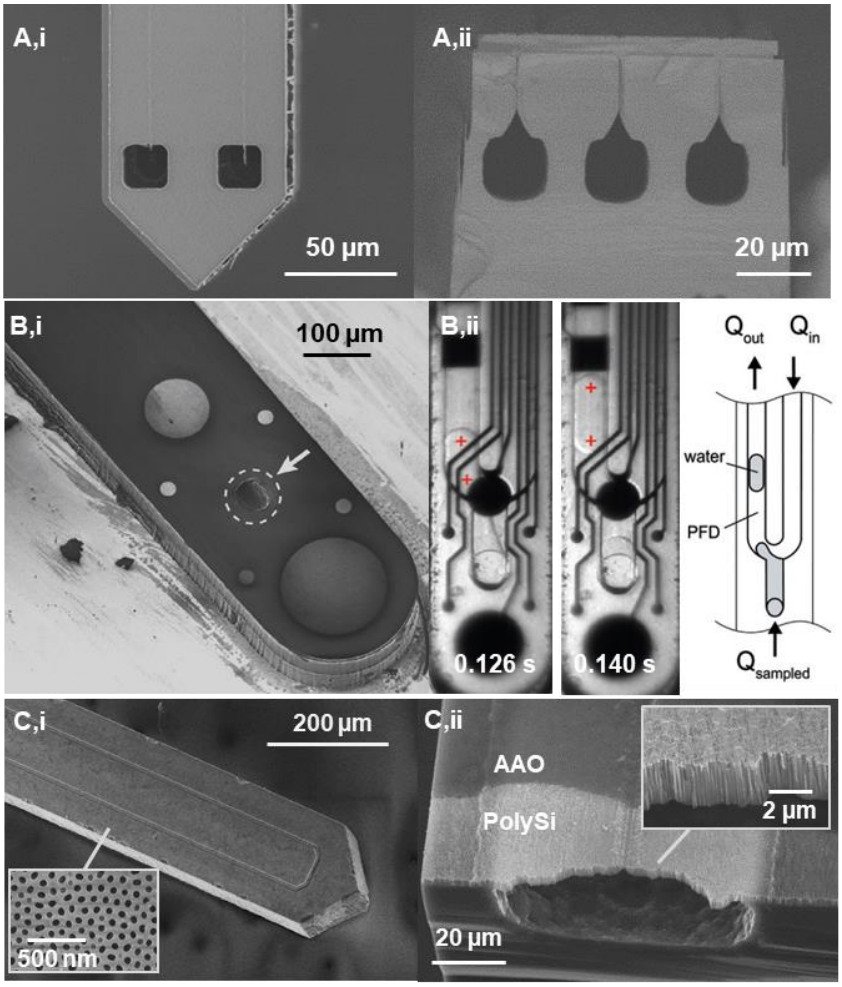

Figure 4

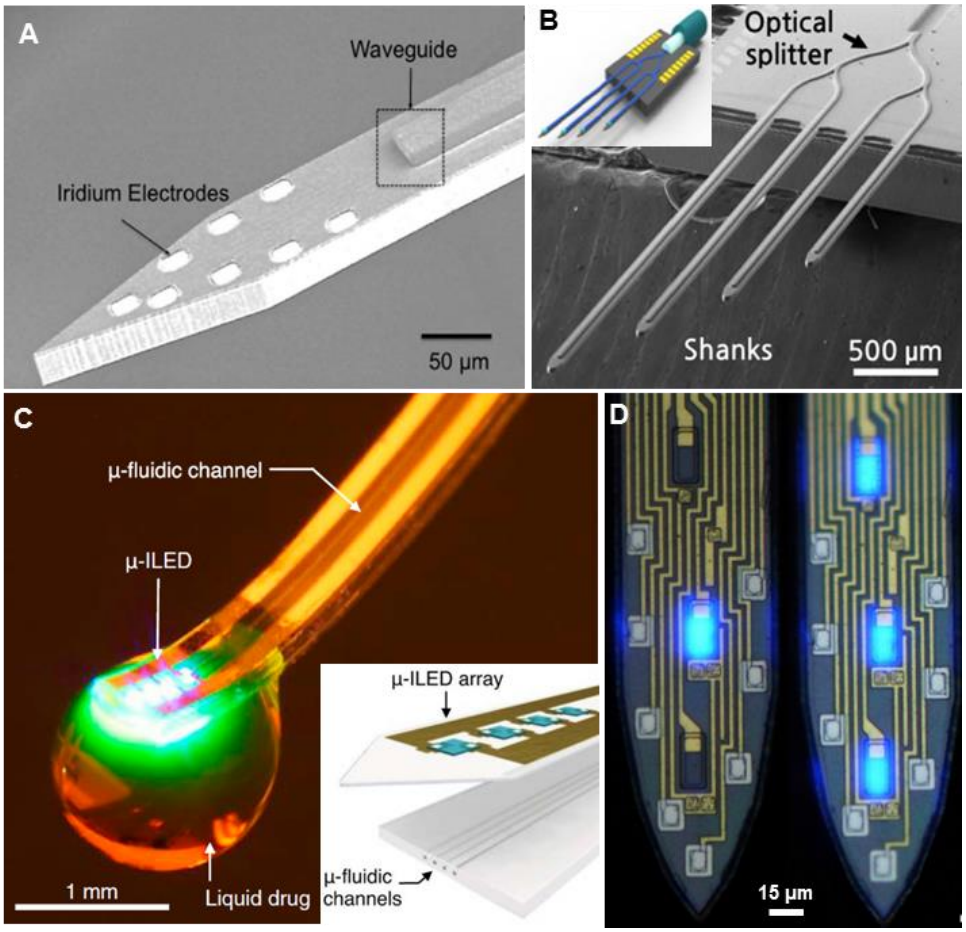

Table 1. Summary of strengths and weaknesses of current in vivo monitoring technology

Techniques	Strengths	Weaknesses
PET	• Non-invasive • Very low LOD (pM to nM)	• Limited spatial resolution (2 - 3 mm) • Limited temporal resolution (several secs to mins) • Require tracers • Limited to immobilized subjects
fMRS	• Non-invasive • Does not require tracers	• Limited spatial resolution (1 mm) • Limited temporal resolution (several secs to mins) • High LOD (mM to µM) • Limited to immobilized subjects
Genetically-encoded biosensors	• Non-invasive • High spatial and temporal resolution (~1 µm, ms to s scale) • Low LOD (nM to µM)	• Difficult to engineer fluorescent markers • Only Glu can be measured in vivo
Electrochemical sensors	• High spatial and temporal resolution (10 - 100 µm, ms to s scale) • Low LOD (nM to µM)	• Limited number of measurable neurochemicals • Limited multiplexing
Sampling methods	• Versatile approach for multiplexed measurement • Very low LOD (pM to nM)	• Limited spatial resolution (100 µm - 4 mm) • Limited temporal resolution (10 s)

Table 2. Summary of microfabricated electrodes for in vivo neurochemical recording

Ref.#	Substrate	WE	Integrated RE	Insulator	Probe size (w × t, l)	# of E	Surface area of E	Target analyte	Surface modification	Detection	Sensitivity	LOD	T_{90}	Brain region
[88]	***Si***	Pt	-	SiO_2, Si_3N_4	90 µm × 15 µm, 6 mm	7	450 μm^2	DA	Nafion	Amp	10 pA/µM	200 nM		Striatum
[89]		Pt	-	SiO_2	120 µm × 150µm, 6 mm	4	4800 μm^2	Glu	1) polypyrrole, 2) Nafion, 3)GluX+BSA+GA	Amp	2.5 pA/µM	790 nM	~1 s	Striatum
[90]		Pt	IrOx	SiO_2	120 µm × 150µm, 6 mm	4	4800 μm^2	Glu	1) polypyrrole, 2) Nafion, 3)GluX+BSA+GA	Amp	7.3 pA/µM	320 nM		Striatum
[91,92]		Pt	Ag/AgCl	SiO_2, Si_3N_4	100 µm × 80µm, 6.5 mm	4 × 4	7500 μm^2	Glu	1) APTES, 2) GluX+BSA+GA, 3) m-polyphenylenediamine	Amp	7.1 pA/µM	420 nM	6 s	Cortex
								Ch	1) APTES, 2) ChoX+BSA+GA, 3) m-polyphenylenediamine	Amp	9.9 pA/µM	300 nM	6 s	
[93]		Pyrolized C	-	Si_3N_4	100 µm × 15µm, 6 mm	4, 16	1000 μm^2	DA	None	FSCV	14.5 nA/µM			Striatum
[94]		Pt	-	SiO_2, SU-8	100 µm × 50µm, 3 mm	3	8000 μm^2	Gluc	1)poly-m-phenylenediamine, 2) GOX+BSA+GA, 3) polyurethane	Amp	11 pA/µM			Cortex
								Lac	1)poly-m-phenylenediamine, 2) LacX+BSA+PEGDE, 3) polyurethane	Amp	3.6 pA/µM			
[95]		Pt	-	SiO_2, Si_3N_4	343 µm × 30µm, 7 mm	8	7500 μm^2	Glu	1) GluX+BSA+GA, 2) 1,3-phenylenediamine	Amp	56 pA/µM	500 nM	< 8 s	Striatum
[96,97]	***Ceramic***	Pt	-	PI	120 µm × 125µm	4	7500 μm^2	Glu	1) Nafion, 2)GluOx+BSA+GA	Amp	17 pA/µM	500 nM	~1 s	Cortex, cerebellum, striatum
[98]		Pt	-	PI	120 µm × 125µm	4	7500 μm^2	Lac	1) Nafion, 2) LacX+BSA+GA, 3)polyurethane	Amp	7.3 pA/µM	78 µM	~5 s	Cortex, striatum
[99]		Pt	-	PI	120 µm × 125µm	4	5000 μm^2	ACh	1)meta-phenylenediamine, 2) ChoX+BSA+GA, 3)hAChE+BSA+GA	Amp	4.7 pA/µM	180 nM	~1 s	Striatum
								Ch	1)meta-phenylenediamine, 2) ChoX+BSA+GA,	Amp				
[100]		Pt	-	PI	120 µm × 125µm	4	5000 μm^2	Gluc	1)meta-phenylenediamine, 2) ChoX+BSA+GA, 3)hAChE+BSA+GA	Amp	1.5 pA/µM	7.8 µM	1.2 s	Hippocampus
[102]	***Polyimide***	Pt	Ag/AgCl	SU-8	500 µm × 100µm, 5.5 mm or 16 mm	4	95000 μm^2	Glu	1)1, 3-diaminobenzene, 2) GluOx+BSA+GA	Amp	205 pA/µM	220 nM	4.9 s	Cortex
								Lac	1) 1, 3-diaminobenzene, 2)LacX + pHEMA hydrogel	Amp	3 pA/µM	2 µM		
[101]		Au	IrOx	PI	700 µm diameter	4		Gluc	1)Pt nanoparticles 2) GOX+BSA+GA	Amp		31 µM		Cortex
[103]	***Glass (temporary)***	C-fiber	-	Parylene	9 µm diameter	8	1000 - 4000 μm^2	DA	None	FSCV	2-50 nA/µM		0.1 s	Striatum

Abbreviations: WE = working electrode; RE = reference electrode; PI = polyimide; (w × t, l) = (wide × thick, long), DA = dopamine, Glu = glutamate, Ch = choline, ACh = acetylcholine, Gluc = glucose, Lac = lactate; GluX = glucose oxidase, BSA = bovine serum albumin, GA = glutaraldehyde, GOX = glucose oxidase, APTES = (3-aminopropyl)triethoxysilane, LacX = lactate oxidase, pHEMA = poly(hydroxyethyl methacrylate, hAChE = human acetylcholinesterase; Amp = Amperometry, FSCV = fast-scan cyclic voltammetry, LOD = limit of detection. T_{90} = response time.

References

[1] D. Purves, G. Augustine, D. Fitzpatrick, W. Hall, A. S. LaMantia, L. White, *Neuroscience*, Sinauer Associates, Sunderland, MA, **2012**.
[2] R. Webster, *Neurotransmitters, Drugs and Brain Function*, John Wiley & Sons, **2001**.
[3] T. Myhrer, *Brain Res. Rev.* **2003**, *41*, 268–287.
[4] W. Schultz, *Trends Neurosci.* **2007**, *30*, 203–210.
[5] R. Cools, A. C. Roberts, T. W. Robbins, *Trends Cogn. Sci.* **2008**, *12*, 31–40.
[6] P. Kása, Z. Rakonczay, K. Gulya, *Prog. Neurobiol.* **1997**, *52*, 511–535.
[7] P. T. Francis, *Int. J. Geriatr. Psychiatry* **2003**, *18*, S15–S21.
[8] P. T. Francis, E. K. Perry, *Mov. Disord.* **2007**, *22*, S351–S357.
[9] P. Barone, *Eur. J. Neurol.* **2010**, *17*, 364–376.
[10] S. H. Fox, R. Chuang, J. M. Brotchie, *Mov. Disord.* **2009**, *24*, 1255–1266.
[11] J. Blesa, S. Przedborski, *Front. Neuroanat.* **2014**, *8*, DOI 10.3389/fnana.2014.00155.
[12] L. F. Barros, J. W. Deitmer, *Brain Res. Rev.* **2010**, *63*, 149–159.
[13] T. C. Glenn, D. F. Kelly, W. J. Boscardin, D. L. McArthur, P. Vespa, M. Oertel, D. A. Hovda, M. Bergsneider, L. Hillered, N. A. Martin, *J. Cereb. Blood Flow Metab.* **2003**, *23*, 1239–1250.
[14] R. Meierhans, M. Béchir, S. Ludwig, J. Sommerfeld, G. Brandi, C. Haberthür, R. Stocker, J. F. Stover, *Crit. Care* **2010**, *14*, R13.
[15] K. L. H. Carpenter, I. Jalloh, P. J. Hutchinson, *Front. Neurosci.* **2015**, *9*, DOI 10.3389/fnins.2015.00112.
[16] N. D. Volkow, M. Morales, *Cell* **2015**, *162*, 712–725.
[17] R. A. Wise, *Neuron* **2002**, *36*, 229–240.
[18] B. J. Venton, R. M. Wightman, *Anal. Chem.* **2003**, *75*, 414 A-421 A.
[19] J. J. Day, M. F. Roitman, R. M. Wightman, R. M. Carelli, *Nat. Neurosci.* **2007**, *10*, 1020–1028.
[20] A. S. Darvesh, R. T. Carroll, W. J. Geldenhuys, G. A. Gudelsky, J. Klein, C. K. Meshul, C. J. Van der Schyf, *Exp Op Drug Disc* **2011**, *6*, 109–127.
[21] R. N. Adams, *Anal. Chem.* **1976**, *48*, 1126A–1138A.
[22] D. L. Robinson, B. J. Venton, M. L. Heien, R. M. Wightman, *Clin. Chem.* **2003**, *49*, 1763–1773.
[23] E. S. Bucher, R. M. Wightman, *Annu. Rev. Anal. Chem.* **2015**, *8*, 239–261.
[24] U. Ungerstedt, in *Meas. Neurotransmitter Release Vivo*, Wiley New York, **1984**, pp. 81–107.
[25] C. J. Watson, B. J. Venton, R. T. Kennedy, *Anal. Chem.* **2006**, *78*, 1391–1399.
[26] B. H. C. Westerink, T. I. F. H. Cremers, *Handbook of Microdialysis: Methods, Applications and Perspectives*, Academic Press, **2007**.
[27] P. Nandi, S. M. Lunte, *Anal. Chim. Acta* **2009**, *651*, 1–14.
[28] R. T. Kennedy, *Curr. Opin. Chem. Biol.* **2013**, *17*, 860–867.
[29] C. A. Owesson-White, J. F. Cheer, M. Beyene, R. M. Carelli, R. M. Wightman, *Proc. Natl. Acad. Sci.* **2008**, *105*, 11957–11962.
[30] L. I. Schmitt, R. E. Sims, N. Dale, P. G. Haydon, *J. Neurosci. Off. J. Soc. Neurosci.* **2012**, *32*, 4417–4425.
[31] D. P. Daberkow, H. D. Brown, K. D. Bunner, S. A. Kraniotis, M. A. Doellman, M. E. Ragozzino, P. A. Garris, M. F. Roitman, *J. Neurosci.* **2013**, *33*, 452–463.
[32] G. Di Chiara, V. Bassareo, S. Fenu, M. A. De Luca, L. Spina, C. Cadoni, E. Acquas, E. Carboni, V. Valentini, D. Lecca, *Neuropharmacology* **2004**, *47*, 227–241.
[33] J.-E. Kang, M. M. Lim, R. J. Bateman, J. J. Lee, L. P. Smyth, J. R. Cirrito, N. Fujiki, S. Nishino, D. M. Holtzman, *Science* **2009**, *326*, 1005–1007.
[34] A. A. Hamid, J. R. Pettibone, O. S. Mabrouk, V. L. Hetrick, R. Schmidt, C. M. Vander Weele, R. T. Kennedy, B. J. Aragona, J. D. Berke, *Nat. Neurosci.* **2016**, *19*, 117–126.

[35] K. T. Kishida, S. G. Sandberg, T. Lohrenz, Y. G. Comair, I. Sáez, P. E. M. Phillips, P. R. Montague, *PLOS ONE* **2011**, *6*, e23291.
[36] S.-Y. Chang, I. Kim, M. P. Marsh, D. P. Jang, S.-C. Hwang, J. J. V. Gompel, S. J. Goerss, C. J. Kimble, K. E. Bennet, P. A. Garris, et al., *Mayo Clin. Proc.* **2012**, *87*, 760–765.
[37] K. T. Kishida, I. Saez, T. Lohrenz, M. R. Witcher, A. W. Laxton, S. B. Tatter, J. P. White, T. L. Ellis, P. E. M. Phillips, P. R. Montague, *Proc. Natl. Acad. Sci.* **2016**, *113*, 200–205.
[38] P. Vespa, M. Prins, E. Ronne-Engstrom, M. Caron, E. Shalmon, D. A. Hovda, N. A. Martin, D. P. Becker, *J. Neurosurg.* **1998**, *89*, 971–982.
[39] R. J. Shannon, K. L. H. Carpenter, M. R. Guilfoyle, A. Helmy, P. J. Hutchinson, *J. Pharmacokinet. Pharmacodyn.* **2013**, *40*, 343–358.
[40] R. Kitagawa, S. Yokobori, A. T. Mazzeo, R. Bullock, *Neurosurg. Clin. N. Am.* **2013**, *24*, 417–426.
[41] M. Fillenz, *Neurosci. Biobehav. Rev.* **2005**, *29*, 949–962.
[42] K. N. Schultz, R. T. Kennedy, *Annu. Rev. Anal. Chem.* **2008**, *1*, 627–661.
[43] M. Perry, Q. Li, R. T. Kennedy, *Anal. Chim. Acta* **2009**, *653*, 1–22.
[44] M. Zhang, P. Yu, L. Mao, *Acc. Chem. Res.* **2012**, *45*, 533–543.
[45] B. Zhang, K. L. Adams, S. J. Luber, D. J. Eves, M. L. Heien, A. G. Ewing, *Anal. Chem.* **2008**, *80*, 1394–1400.
[46] R. Trouillon, A. G. Ewing, *ACS Chem. Biol.* **2014**, *9*, 812–820.
[47] S. Tucci, P. Rada, M. J. Sepúlveda, L. Hernandez, *J. Chromatogr. B. Biomed. Sci. App.* **1997**, *694*, 343–349.
[48] M. L. Heien, A. S. Khan, J. L. Ariansen, J. F. Cheer, P. E. Phillips, K. M. Wassum, R. M. Wightman, *Proc. Natl. Acad. Sci. U. S. A.* **2005**, *102*, 10023–10028.
[49] B. J. Venton, R. M. Wightman, *Synapse* **2007**, *61*, 37–39.
[50] J. P. Bruno, C. Gash, B. Martin, A. Zmarowski, F. Pomerleau, J. Burmeister, P. Huettl, G. A. Gerhardt, *Eur. J. Neurosci.* **2006**, *24*, 2749–2757.
[51] P. Song, O. S. Mabrouk, N. D. Hershey, R. T. Kennedy, *Anal. Chem.* **2012**, *84*, 412–419.
[52] S. M. Ametamey, M. Honer, P. A. Schubiger, *Chem. Rev.* **2008**, *108*, 1501–1516.
[53] I. Nasrallah, J. Dubroff, *Semin. Nucl. Med.* **2013**, *43*, 449–461.
[54] L. Zimmer, A. Luxen, *NeuroImage* **2012**, *61*, 363–370.
[55] D. Schulz, S. Southekal, S. S. Junnarkar, J.-F. Pratte, M. L. Purschke, S. P. Stoll, B. Ravindranath, S. H. Maramraju, S. Krishnamoorthy, F. A. Henn, et al., *Nat. Methods* **2011**, *8*, 347–352.
[56] R. Yao, R. Lecomte, E. S. Crawford, *J. Nucl. Med. Technol.* **2012**, *40*, 157–165.
[57] D. F. Wong, J. R. Brašić, H. S. Singer, D. J. Schretlen, H. Kuwabara, Y. Zhou, A. Nandi, M. A. Maris, M. Alexander, W. Ye, et al., *Neuropsychopharmacology* **2008**, *33*, 1239–1251.
[58] L. Tuominen, L. Nummenmaa, L. Keltikangas-Järvinen, O. Raitakari, J. Hietala, *Hum. Brain Mapp.* **2014**, *35*, 1875–1884.
[59] C. Y. Sander, J. M. Hooker, C. Catana, M. D. Normandin, N. M. Alpert, G. M. Knudsen, W. Vanduffel, B. R. Rosen, J. B. Mandeville, *Proc. Natl. Acad. Sci.* **2013**, *110*, 11169–11174.
[60] H. Zhu, P. B. Barker, in *Magn. Reson. Neuroimaging* (Eds.: M. Modo, J.W.M. Bulte), Humana Press, Totowa, NJ, **2011**, pp. 203–226.
[61] J. M. N. Duarte, H. Lei, V. Mlynárik, R. Gruetter, *NeuroImage* **2012**, *61*, 342–362.
[62] A. Gussew, R. Rzanny, M. Erdtel, H. C. Scholle, W. A. Kaiser, H. J. Mentzel, J. R. Reichenbach, *NeuroImage* **2010**, *49*, 1895–1902.
[63] N. A. J. Puts, R. A. E. Edden, *Prog. Nucl. Magn. Reson. Spectrosc.* **2012**, *60*, 29–41.
[64] I. Betina Ip, A. Berrington, A. T. Hess, A. J. Parker, U. E. Emir, H. Bridge, *Neuroimage* **2017**, *155*, 113–119.

[65] J. S. Marvin, B. G. Borghuis, L. Tian, J. Cichon, M. T. Harnett, J. Akerboom, A. Gordus, S. L. Renninger, T.-W. Chen, C. I. Bargmann, et al., *Nat. Methods* **2013**, *10*, 162–170.
[66] R. Liang, G. J. Broussard, L. Tian, *ACS Chem. Neurosci.* **2015**, *6*, 84–93.
[67] M. Z. Lin, M. J. Schnitzer, *Nat. Neurosci.* **2016**, *19*, 1142–1153.
[68] D. L. Robinson, A. Hermans, A. T. Seipel, R. M. Wightman, *Chem. Rev.* **2008**, *108*, 2554–2584.
[69] J. Wang, *Chem. Rev.* **2008**, *108*, 814–825.
[70] G. S. Wilson, M. A. Johnson, *Chem. Rev.* **2008**, *108*, 2462–2481.
[71] A. Weltin, J. Kieninger, G. A. Urban, *Anal. Bioanal. Chem.* **2016**, *408*, 4503–4521.
[72] D. L. Robinson, R. M. Wightman, in *Electrochem. Methods Neurosci.* (Eds.: A.C. Michael, L.M. Borland), CRC Press/Taylor & Francis, Boca Raton (FL), **2007**.
[73] K. Jackowska, P. Krysinski, *Anal. Bioanal. Chem.* **2013**, *405*, 3753–3771.
[74] R. M. Wightman, M. L. A. V. Heien, K. M. Wassum, L. A. Sombers, B. J. Aragona, A. S. Khan, J. L. Ariansen, J. F. Cheer, P. E. M. Phillips, R. M. Carelli, *Eur. J. Neurosci.* **2007**, *26*, 2046–2054.
[75] J. J. Clark, S. G. Sandberg, M. J. Wanat, J. O. Gan, E. A. Horne, A. S. Hart, C. A. Akers, J. G. Parker, I. Willuhn, V. Martinez, et al., *Nat. Methods* **2010**, *7*, 126–129.
[76] S. F. Dressman, J. L. Peters, A. C. Michael, *J. Neurosci. Methods* **2002**, *119*, 75–81.
[77] R. A. Saylor, S. M. Lunte, *J. Chromatogr. A* **2015**, *1382*, 48–64.
[78] S. Kottegoda, I. Shaik, S. A. Shippy, *J. Neurosci. Methods* **2002**, *121*, 93–101.
[79] T. R. Slaney, J. Nie, N. D. Hershey, P. K. Thwar, J. Linderman, M. A. Burns, R. T. Kennedy, *Anal. Chem.* **2011**, *83*, 5207–5213.
[80] C. M. Mitala, Y. Wang, L. M. Borland, M. Jung, S. Shand, S. Watkins, S. G. Weber, A. C. Michael, *J. Neurosci. Methods* **2008**, *174*, 177–185.
[81] K. D. Wise, *IEEE Eng. Med. Biol. Mag.* **2005**, *24*, 22–29.
[82] M. HajjHassan, V. Chodavarapu, S. Musallam, *Sensors* **2008**, *8*, 6704–6726.
[83] Z. Fekete, *Sens. Actuators B Chem.* **2015**, *215*, 300–315.
[84] J. P. Seymour, F. Wu, K. D. Wise, E. Yoon, *Microsyst. Nanoeng.* **2017**, *3*, 16066.
[85] K. D. Wise, D. J. Anderson, J. F. Hetke, D. R. Kipke, K. Najafi, *Proc. IEEE* **2004**, *92*, 76–97.
[86] B. C. Raducanu, R. F. Yazicioglu, C. M. Lopez, M. Ballini, J. Putzeys, S. Wang, A. Andrei, V. Rochus, M. Welkenhuysen, N. van Helleputte, et al., *Sensors* **2017**, *17*, 2388.
[87] D. Grieshaber, R. MacKenzie, J. Voeroes, E. Reimhult, *Sensors* **2008**, *8*, 1400–1458.
[88] M. D. Johnson, R. K. Franklin, M. D. Gibson, R. B. Brown, D. R. Kipke, *J. Neurosci. Methods* **2008**, *174*, 62–70.
[89] K. M. Wassum, V. M. Tolosa, J. Wang, E. Walker, H. G. Monbouquette, N. T. Maidment, *Sensors* **2008**, *8*, 5023–5036.
[90] V. M. Tolosa, K. M. Wassum, N. T. Maidment, H. G. Monbouquette, *Biosens. Bioelectron.* **2013**, *42*, 256–260.
[91] O. Frey, T. Holtzman, R. M. McNamara, D. E. H. Theobald, P. D. van der Wal, N. F. de Rooij, J. W. Dalley, M. Koudelka-Hep, *Biosens. Bioelectron.* **2010**, *26*, 477–484.
[92] O. Frey, T. Holtzman, R. M. McNamara, D. E. H. Theobald, P. D. van der Wal, N. F. de Rooij, J. W. Dalley, M. Koudelka-Hep, *Sens. Actuators B Chem.* **2011**, *154*, 96–105.
[93] M. K. Zachek, J. Park, P. Takmakov, R. M. Wightman, G. S. McCarty, *The Analyst* **2010**, *135*, 1556.
[94] N. Vasylieva, S. Marinesco, D. Barbier, A. Sabac, *Biosens. Bioelectron.* **2015**, *72*, 148–155.
[95] W. Wei, Y. Song, L. Wang, S. Zhang, J. Luo, S. Xu, X. Cai, *Microsyst. Nanoeng.* **2015**, *1*, 15002.
[96] J. J. Burmeister, F. Pomerleau, M. Palmer, B. K. Day, P. Huettl, G. A. Gerhardt, *J. Neurosci. Methods* **2002**, *119*, 163–171.

[97] B. K. Day, F. Pomerleau, J. J. Burmeister, P. Huettl, G. A. Gerhardt, *J. Neurochem.* **2006**, *96*, 1626–1635.
[98] J. J. Burmeister, M. Palmer, G. A. Gerhardt, *Biosens. Bioelectron.* **2005**, *20*, 1772–1779.
[99] J. J. Burmeister, F. Pomerleau, P. Huettl, C. R. Gash, C. E. Werner, J. P. Bruno, G. A. Gerhardt, *Biosens. Bioelectron.* **2008**, *23*, 1382–1389.
[100] C. F. Lourenço, A. Ledo, J. Laranjinha, G. A. Gerhardt, R. M. Barbosa, *Sens. Actuators B Chem.* **2016**, *237*, 298–307.
[101] C. Li, K. Limnuson, Z. Wu, A. Amin, A. Narayan, E. V. Golanov, C. H. Ahn, J. A. Hartings, R. K. Narayan, *Biosens. Bioelectron.* **2016**, *77*, 62–68.
[102] A. Weltin, J. Kieninger, B. Enderle, A.-K. Gellner, B. Fritsch, G. A. Urban, *Biosens. Bioelectron.* **2014**, *61*, 192–199.
[103] H. N. Schwerdt, M. J. Kim, S. Amemori, D. Homma, T. Yoshida, H. Shimazu, H. Yerramreddy, E. Karasan, R. Langer, A. M. Graybiel, et al., *Lab Chip* **2017**, *17*, 1104–1115.
[104] M. K. Zachek, P. Takmakov, B. Moody, R. M. Wightman, G. S. McCarty, *Anal. Chem.* **2009**, *81*, 6258–6265.
[105] R. A. Green, N. H. Lovell, G. G. Wallace, L. A. Poole-Warren, *Biomaterials* **2008**, *29*, 3393–3399.
[106] J.-W. Jeong, G. Shin, S. I. Park, K. J. Yu, L. Xu, J. A. Rogers, *Neuron* **2015**, *86*, 175–186.
[107] R. Green, M. R. Abidian, *Adv. Mater.* **2015**, *27*, 7620–7637.
[108] G. Baranauskas, E. Maggiolini, E. Castagnola, A. Ansaldo, A. Mazzoni, G. N. Angotzi, A. Vato, D. Ricci, S. Panzeri, L. Fadiga, *J. Neural Eng.* **2011**, *8*, 066013.
[109] C. B. Jacobs, M. J. Peairs, B. J. Venton, *Anal. Chim. Acta* **2010**, *662*, 105–127.
[110] C. Yang, M. E. Denno, P. Pyakurel, B. J. Venton, *Anal. Chim. Acta* **2015**, *887*, 17–37.
[111] Y. Liu, X. Dong, P. Chen, *Chem. Soc. Rev.* **2012**, *41*, 2283–2307.
[112] M. Deng, X. Yang, M. Silke, W. Qiu, M. Xu, G. Borghs, H. Chen, *Sens. Actuators B Chem.* **2011**, *158*, 176–184.
[113] C. L. Weaver, H. Li, X. Luo, X. T. Cui, *J Mater Chem B* **2014**, *2*, 5209–5219.
[114] G. Márton, I. Bakos, Z. Fekete, I. Ulbert, A. Pongrácz, *J. Mater. Sci. Mater. Med.* **2014**, *25*, 931–940.
[115] G. S. Wilson, Y. Hu, *Chem. Rev.* **2000**, *100*, 2693–2704.
[116] M. Suzuki, H. Akaguma, *Sens. Actuators B Chem.* **2000**, *64*, 136–141.
[117] P. M. Talauliker, D. A. Price, J. J. Burmeister, S. Nagari, J. E. Quintero, F. Pomerleau, P. Huettl, J. T. Hastings, G. A. Gerhardt, *J. Neurosci. Methods* **2011**, *198*, 222–229.
[118] M. Yuqing, C. Jianrong, W. Xiaohua, *Trends Biotechnol.* **2004**, *22*, 227–231.
[119] F. Laermer, A. Schilp, *Method of Anisotropically Etching Silicon*, **1996**, 5501893.
[120] B. Wu, A. Kumar, S. Pamarthy, *J. Appl. Phys.* **2010**, *108*, 051101.
[121] K. Najafi, K. D. Wise, T. Mochizuki, *IEEE Trans. Electron Devices* **1985**, *32*, 1206–1211.
[122] P. Norlin, M. Kindlundh, A. Mouroux, K. Yoshida, U. G. Hofmann, *J. Micromechanics Microengineering* **2002**, *12*, 414.
[123] K. C. Cheung, K. Djupsund, Y. Dan, L. P. Lee, *J. Microelectromechanical Syst.* **2003**, *12*, 179–184.
[124] K. D. Wise, A. M. Sodagar, Y. Yao, M. N. Gulari, G. E. Perlin, K. Najafi, *Proc. IEEE* **2008**, *96*, 1184–1202.
[125] S. Herwik, O. Paul, P. Ruther, *J. Microelectromechanical Syst.* **2011**, *20*, 791–793.
[126] Z. Fekete, *Microsyst. Technol.* **2015**, *21*, 341–344.
[127] J. J. Burmeister, K. Moxon, G. A. Gerhardt, *Anal. Chem.* **2000**, *72*, 187–192.
[128] J. J. Burmeister, G. A. Gerhardt, *Anal. Chem.* **2001**, *73*, 1037–1042.
[129] E. C. Rutherford, F. Pomerleau, P. Huettl, I. Strömberg, G. A. Gerhardt, *J. Neurochem.* **2007**, *102*, 712–722.

[130] S. P. Lacour, S. Benmerah, E. Tarte, J. FitzGerald, J. Serra, S. McMahon, J. Fawcett, O. Graudejus, Z. Yu, B. Morrison, *Med. Biol. Eng. Comput.* **2010**, *48*, 945–954.
[131] B. J. Kim, E. Meng, *J. Micromechanics Microengineering* **2016**, *26*, 013001.
[132] Z. Fekete, A. Pongrácz, *Sens. Actuators B Chem.* **2017**, *243*, 1214–1223.
[133] A. A. Sharp, H. V. Panchawagh, A. Ortega, R. Artale, S. Richardson-Burns, D. S. Finch, K. Gall, R. L. Mahajan, D. Restrepo, *J. Neural Eng.* **2006**, *3*, L23.
[134] T. Ware, D. Simon, D. E. Arreaga-Salas, J. Reeder, R. Rennaker, E. W. Keefer, W. Voit, *Adv. Funct. Mater.* **2012**, *22*, 3470–3479.
[135] D.-H. Do, M. Ecker, W. E. Voit, *ACS Omega* **2017**, *2*, 4604–4611.
[136] T. Suzuki, K. Mabuchi, S. Takeuchi, in *Neural Eng. 2003 Conf. Proc. First Int. IEEE EMBS Conf. On*, IEEE, **2003**, pp. 154–156.
[137] B. J. Kim, J. T. W. Kuo, S. A. Hara, C. D. Lee, L. Yu, C. A. Gutierrez, T. Q. Hoang, V. Pikov, E. Meng, *J. Neural Eng.* **2013**, *10*, 045002.
[138] L. W. Tien, F. Wu, M. D. Tang-Schomer, E. Yoon, F. G. Omenetto, D. L. Kaplan, *Adv. Funct. Mater.* **2013**, *23*, 3185–3193.
[139] A. Lecomte, V. Castagnola, E. Descamps, L. Dahan, M. C. Blatché, T. M. Dinis, E. Leclerc, C. Egles, C. Bergaud, *J. Micromechanics Microengineering* **2015**, *25*, 125003.
[140] A. K. Dengler, R. M. Wightman, G. S. McCarty, *Anal. Chem.* **2015**, *87*, 10556–10564.
[141] M. O. Heuschkel, M. Fejtl, M. Raggenbass, D. Bertrand, P. Renaud, *J. Neurosci. Methods* **2002**, *114*, 135–148.
[142] Z. Zhao, R. Gong, H. Huang, J. Wang, *Sensors* **2016**, *16*, DOI 10.3390/s16060880.
[143] J. Chen, K. D. Wise, J. F. Hetke, S. C. Bledsoe, *Biomed. Eng. IEEE Trans. On* **1997**, *44*, 760–769.
[144] H. Shin, H. J. Lee, U. Chae, H. Kim, J. Kim, N. Choi, J. Woo, Y. Cho, C. J. Lee, E.-S. Yoon, et al., *Lab Chip* **2015**, *15*, 3730–3737.
[145] A. Altuna, E. Bellistri, E. Cid, P. Aivar, B. Gal, J. Berganzo, G. Gabriel, A. Guimerà, R. Villa, L. J. Fernández, et al., *Lab. Chip* **2013**, *13*, 1422.
[146] M. J. de Boer, R. W. Tjerkstra, J. W. Berenschot, H. V. Jansen, G. J. Burger, J. G. E. Gardeniers, M. Elwenspoek, A. van den Berg, *Microelectromechanical Syst. J. Of* **2000**, *9*, 94–103.
[147] Z. Fekete, A. Pongrácz, P. Fürjes, G. Battistig, *Microsyst. Technol.* **2012**, *18*, 353–358.
[148] J. Y. Sim, M. P. Haney, S. I. Park, J. G. McCall, J.-W. Jeong, *Lab Chip* **2017**, *17*, 1406–1435.
[149] A. Pongrácz, Z. Fekete, G. Márton, Z. Bérces, I. Ulbert, P. Fürjes, *Sens. Actuators B Chem.* **2013**, *189*, 97–105.
[150] S. Spieth, A. Schumacher, T. Holtzman, P. D. Rich, D. E. Theobald, J. W. Dalley, R. Nouna, S. Messner, R. Zengerle, *Biomed. Microdevices* **2012**, *14*, 799–809.
[151] W. H. Lee, T. R. Slaney, R. W. Hower, R. T. Kennedy, *Anal. Chem.* **2013**, *85*, 3828–3831.
[152] U. Chae, H. Shin, H. Lee, J. Lee, N. Choi, Y. J. Lee, S. H. Lee, J. Woo, Y. Cho, E.-S. Yoon, et al., in *IEEE MEMS*, Shanghai, China, **2016**, pp. 329–332.
[153] G. Petit-Pierre, A. Bertsch, P. Renaud, *Lab Chip* **2016**, *16*, 917–924.
[154] S. P. Adiga, C. Jin, L. A. Curtiss, N. A. Monteiro-Riviere, R. J. Narayan, *Wiley Interdiscip. Rev. Nanomed. Nanobiotechnol.* **2009**, *1*, 568–581.
[155] S. Metz, C. Trautmann, A. Bertsch, P. Renaud, in *Micro Electro Mech. Syst. 2002 Fifteenth IEEE Int. Conf. On*, IEEE, **2002**, pp. 81–84.
[156] H. D. Tong, H. V. Jansen, V. J. Gadgil, C. G. Bostan, E. Berenschot, C. J. M. van Rijn, M. Elwenspoek, *Nano Lett.* **2004**, *4*, 283–287.
[157] C. C. Striemer, T. R. Gaborski, J. L. McGrath, P. M. Fauchet, *Nature* **2007**, *445*, 749–753.
[158] J. D. Zahn, D. Trebotich, D. Liepmann, *Biomed. Microdevices* **2005**, *7*, 59–69.

[159] N. Tas, T. Sonnerberg, H. Jansen, R. Legtenberg, M. Elwenspoek, *J Micromech Microeng* **1996**, *6*, 385–397.
[160] J. Liang, H. Chik, A. Yin, J. Xu, *J. Appl. Phys.* **2002**, *91*, 2544–2546.
[161] G. E. J. Poinern, N. Ali, D. Fawcett, *Materials* **2011**, *4*, 487–526.
[162] A. Santos, T. Kumeria, D. Losic, *TrAC Trends Anal. Chem.* **2013**, *44*, 25–38.
[163] W. H. Lee, T. Ngernsutivorakul, O. S. Mabrouk, J.-M. T. Wong, C. E. Dugan, S. S. Pappas, H. J. Yoon, R. T. Kennedy, *Anal. Chem.* **2016**, *88*, 1230–1237.
[164] S. G. Taylor, F. R. S, *Proc R Soc Lond A* **1953**, *219*, 186–203.
[165] B. W. Boyd, S. R. Witowski, R. T. Kennedy, *Anal. Chem.* **2000**, *72*, 865–871.
[166] S. Parrot, V. Sauvinet, V. Riban, A. Depaulis, B. Renaud, L. Denoroy, *J. Neurosci. Methods* **2004**, *140*, 29–38.
[167] B. H. Huynh, B. A. Fogarty, R. S. Martin, S. M. Lunte, *Anal. Chem.* **2004**, *76*, 6440–6447.
[168] T. Thorsen, R. W. Roberts, F. H. Arnold, S. R. Quake, *Phys. Rev. Lett.* **2001**, *86*, 4163–4166.
[169] D. Chen, W. Du, Y. Liu, W. Liu, A. Kuznetsov, F. E. Mendez, L. H. Philipson, R. F. Ismagilov, *Proc. Natl. Acad. Sci.* **2008**, *105*, 16843–16848.
[170] L. Shang, Y. Cheng, Y. Zhao, *Chem. Rev.* **2017**, *117*, 7964–8040.
[171] E. Y. Basova, F. Foret, *The Analyst* **2015**, *140*, 22–38.
[172] C. A. Croushore, J. V. Sweedler, *Lab. Chip* **2013**, *13*, 1666.
[173] Y. Zhu, Q. Fang, *Anal. Chim. Acta* **2013**, *787*, 24–35.
[174] M. Wang, G. T. Roman, M. L. Perry, R. T. Kennedy, *Anal. Chem.* **2009**, *81*, 9072–9078.
[175] M. Wang, T. Slaney, O. Mabrouk, R. T. Kennedy, *J. Neurosci. Methods* **2010**, *190*, 39–48.
[176] P. Song, N. D. Hershey, O. S. Mabrouk, T. R. Slaney, R. T. Kennedy, *Anal. Chem.* **2012**, *84*, 4659–4664.
[177] Q. Li, J. Pei, P. Song, R. T. Kennedy, *Anal. Chem.* **2010**, *82*, 5260–5267.
[178] D. C. Gale, R. D. Smith, *Rapid Commun. Mass Spectrom.* **1993**, *7*, 1017–1021.
[179] M. Wilm, M. Mann, *Anal. Chem.* **1996**, *68*, 1–8.
[180] G. T. T. Gibson, S. M. Mugo, R. D. Oleschuk, *Mass Spectrom. Rev.* **2009**, *28*, 918–936.
[181] E. Boyden, *F1000 Biol. Rep.* **2011**, *3*, DOI 10.3410/B3-11.
[182] A. Guru, R. J. Post, Y.-Y. Ho, M. R. Warden, *Int. J. Neuropsychopharmacol.* **2015**, *18*, DOI 10.1093/ijnp/pyv079.
[183] S. K. Mohanty, V. Lakshminarayananan, *J. Mod. Opt.* **2015**, *62*, 949–970.
[184] O. Yizhar, L. E. Fenno, T. J. Davidson, M. Mogri, K. Deisseroth, *Neuron* **2011**, *71*, 9–34.
[185] F. Zhang, V. Gradinaru, A. R. Adamantidis, R. Durand, R. D. Airan, L. de Lecea, K. Deisseroth, *Nat. Protoc.* **2010**, *5*, 439–456.
[186] S. Parrot, L. Denoroy, B. Renaud, C. Benetollo, *ACS Chem. Neurosci.* **2015**, *6*, 948–950.
[187] M. E. Carter, O. Yizhar, S. Chikahisa, H. Nguyen, A. Adamantidis, S. Nishino, K. Deisseroth, L. de Lecea, *Nat. Neurosci.* **2010**, *13*, 1526–1533.
[188] C. E. Bass, V. P. Grinevich, D. Gioia, J. D. Day-Brown, K. D. Bonin, G. D. Stuber, J. L. Weiner, E. A. Budygin, *Front. Behav. Neurosci.* **2013**, *7*, DOI 10.3389/fnbeh.2013.00173.
[189] B. Fan, W. Li, *Lab Chip* **2015**, *15*, 3838–3855.
[190] H. Zhao, *Int. J. Mol. Sci.* **2017**, *18*, 1751.
[191] S. B. Goncalves, J. F. Ribeiro, A. F. Silva, R. M. Costa, J. H. Correia, *J. Neural Eng.* **2017**, *14*, 041001.
[192] M. T. Alt, E. Fiedler, L. Rudmann, J. S. Ordonez, P. Ruther, T. Stieglitz, *Proc. IEEE* **2017**, *105*, 101–138.
[193] L. Hoffman, A. Subramanian, P. Helin, B. D. Bois, R. Baets, P. V. Dorpe, G. Gielen, R. Puers, D. Braeken, *IEEE Photonics J.* **2016**, *8*, 1–11.
[194] A. N. Zorzos, E. S. Boyden, C. G. Fonstad, *Opt. Lett.* **2010**, *35*, 4133–4135.

[195] K. Kampasi, E. Stark, J. Seymour, K. Na, H. G. Winful, G. Buzsáki, K. D. Wise, E. Yoon, *Sci. Rep.* **2016**, *6*, DOI 10.1038/srep30961.
[196] F. Wu, E. Stark, M. Im, I.-J. Cho, E.-S. Yoon, G. Buzsáki, K. D. Wise, E. Yoon, *J. Neural Eng.* **2013**, *10*, 056012.
[197] E. Fiedler, N. Haas, T. Stieglitz, in *2014 36th Annu. Int. Conf. IEEE Eng. Med. Biol. Soc.*, **2014**, pp. 438–441.
[198] Y. Son, H. Jenny Lee, J. Kim, H. Shin, N. Choi, C. Justin Lee, E. S. Yoon, E. Yoon, K. D. Wise, T. G. Kim, et al., *Sci. Rep.* **2015**, *5*, DOI 10.1038/srep15466.
[199] Y. Son, H. J. Lee, J. Kim, C. J. Lee, E. S. Yoon, T. G. Kim, I. J. Cho, in *2015 28th IEEE Int. Conf. Micro Electro Mech. Syst. MEMS*, **2015**, pp. 158–161.
[200] J. W. Jeong, J. G. McCall, G. Shin, Y. Zhang, R. Al-Hasani, M. Kim, S. Li, J. Y. Sim, K. I. Jang, Y. Shi, et al., *Cell* **2015**, *162*, 662–674.
[201] T. I. Kim, J. G. McCall, Y. H. Jung, X. Huang, E. R. Siuda, Y. Li, J. Song, Y. M. Song, H. A. Pao, R. H. Kim, et al., *Science* **2013**, *340*, 211–216.
[202] M. Schwaerzle, K. Seidl, U. T. Schwarz, O. Paul, P. Ruther, in *2013 IEEE 26th Int. Conf. Micro Electro Mech. Syst. MEMS*, **2013**, pp. 1029–1032.
[203] M. Schwaerzle, O. Paul, P. Ruther, *J. Micromechanics Microengineering* **2017**, *27*, 065004.
[204] R. Scharf, T. Tsunematsu, N. McAlinden, M. D. Dawson, S. Sakata, K. Mathieson, *Sci. Rep.* **2016**, *6*, DOI 10.1038/srep28381.
[205] F. Wu, E. Stark, P. C. Ku, K. D. Wise, G. Buzsáki, E. Yoon, *Neuron* **2015**, *88*, 1136–1148.